



# Physical and mechanical properties of compression molded and solution casting soybean protein concentrate based films



Emiliano M. Ciannamea\*, Pablo M. Stefani, Roxana A. Ruseckaite

*Instituto de Investigaciones en Ciencia y Tecnología de Materiales (INTEMA), Av. J.B. Justo 4302, 7600 Mar del Plata, Argentina*

## ARTICLE INFO

### Article history:

Received 27 September 2013

Accepted 4 December 2013

### Keywords:

Soybean protein concentrate  
Film  
Compression molding  
Mechanical and barrier properties

## ABSTRACT

Soybean protein concentrate-based films plasticized by glycerol were obtained by two processing methods: intensive mixing followed by compression molding and solution-casting. Film forming conditions such as molding temperature, molding pressure, drying conditions as well as glycerol level were determined. The effect of the forming method on the physical and mechanical properties of the resultant films was analyzed in terms of color, light transmission, tensile properties, water solubility and water vapor and oxygen barrier properties. Thermo-pressed soy protein concentrate films were significantly more transparent, less soluble, more stretchable and had lower water vapor permeability but greater oxygen permeability coefficient than solution casting films at the same plasticizer level. These results were associated with the intermolecular forces involved in the formation of the films. Hydrophobic interactions and hydrogen bonding dominated the formation solution-casting films, whereas disulphide bonding played a more important role in the formation of compression molded films, as revealed by solubility of obtained films in denaturing solutions and infrared spectroscopy. This study demonstrates that forming process plays a major role in determining the final properties of soy protein concentrate-based films and reveals the possibility of soy protein concentrate-glycerol mixtures to be transformed through thermo-mechanical processing into biodegradable films with potential application in food packaging.

© 2013 Elsevier Ltd. All rights reserved.

## 1. Introduction

Biopolymers extracted directly from biomass, such as polysaccharides and proteins, have received much attention in recent years for the development of biodegradable materials for food packaging and are considered as potential substitutes of non-biodegradable polymers derived from oil, given their renewable origin and biodegradability (Song, Tang, Wang, & Wang, 2011). Among biopolymers, animal and vegetable proteins are of great interest for the production of food packaging films because of their relatively low cost, high availability as byproducts of food industry and agriculture and inherent biodegradability (Janjarasskul & Krochta, 2010; Mangavel et al., 2004; Paetau, Chen, & Jane, 1994; Reddy & Yang, 2013). An additional advantage is that proteins can be processed by diverse methods such as dissolution-solvent evaporation or thermo-mechanical methods to produce films with excellent oxygen barrier properties and suitable mechanical

properties (Guerrero, Retegi, Gabilondo, & de la Caba, 2010; Hernandez-Izquierdo & Krochta, 2008; Krishna, Nindo, & Min, 2012; Mangavel et al., 2004; Reddy & Yang, 2013; Song et al., 2011).

Particularly, soy proteins are an interesting alternative for obtaining environmentally friendly materials. These proteins, in addition to being an abundant and renewable resource with high biodegradability, arouse further interest in Argentina, the third largest producer of soybeans after the United States and Brazil, with 48.8 million tons harvested in 2011. According to official data, the majority of soybean harvest in Argentina is used for the production of flour and oil, 28.6 and 7.1 million tons in 2011, respectively, exporting almost the total, making the country the largest global exporter of these products (Ministry of Agriculture, 2013). Considering that recycling rate of soybean protein into added value products other than food systems, such as adhesives and plastics is constantly increasing there is a great need to investigate new industrial uses for this protein.

Soy proteins mainly consist of four globulin fractions, characterized by the ultracentrifuge sedimentation rates: 2S, 7S, 11S and 15S, expressed in Svedberg units. Among them, the major fractions are glycinin (11S) and conglycinin (7S), representing 31% and 37% of the protein, respectively (Hettiarachchy & Eswaranandam, 2005;

\* Corresponding author. Tel.: +54 (0)2234816600.

E-mail addresses: [emiliano@fi.mdp.edu.ar](mailto:emiliano@fi.mdp.edu.ar), [emilianociannamea@gmail.com](mailto:emilianociannamea@gmail.com) (E.M. Ciannamea).

Kunte, Gennadios, Cuppett, Hanna, & Weller, 1997). Soy protein is available in various commercial forms, such as soybean flour (SF), soy protein concentrate (SPC) and soy protein isolate (SPI) (Song et al., 2011). SF contains about 40–60% protein, combined with fats and carbohydrates. SPC contains about 60–70% protein, a polysaccharide fraction (8–15%) mainly composed of cellulose and pectic polysaccharides (linear hetero-polysaccharides containing free or esterified units based on galacturonic acid) and minor components such as fats (1%), fibers (1–3%) and ashes (3–5%). SPI contains more than 90% of protein (Janjarasskul & Krochta, 2010; Singh, Kumar, Sabapathy, & Bawa, 2008) and is the most widely soybean product used for film processing (Cunningham, Ogale, Dawson, & Acton, 2000; Kokoszka, Debeaufort, Hambleton, Lenart, & Voilley, 2010; Kunte et al., 1997; Paetau et al., 1994; Rhim, Gennadios, Handa, Weller, & Hanna, 2000; Rhim, Gennadios, Weller, Carole, & Hanna, 1998). However, SPI is relatively expensive for the potential production of materials on a large scale in comparison with SPC.

The functional properties of protein films are determined by their microstructure, which strongly depend on the protein structure and the processing method. Protein–protein interactions involved in the generation of the film will define the final properties. The type and number of interactions (electrostatic, hydrophobic, hydrogen bonding and disulfide bridges) will be established by amino acid composition, the average molar mass and the type and variables of the processing technology used to obtain the film. Broadly, two technologies are used to process proteins: the wet and dry methods (Hernandez-Izquierdo & Krochta, 2008; Reddy & Yang, 2013). Wet method (solution casting) first involves the dispersion or solubilization of the protein in a solvent and in a second step the suspension or film-forming solution is placed in a suitable mold and the solvent is evaporated under controlled conditions (Kunte et al., 1997; Mangavel et al., 2004). During this process the primarily polymer–polymer interactions are set, resulting in a stable three-dimensional network (Hernandez-Izquierdo & Krochta, 2008; Reddy & Yang, 2013). The result of the casting process depends mainly on the mixing conditions: temperature, time, type and concentration of solvent, plasticizer and pH, and the drying relative humidity and temperature (Gällstedt, Mattozzi, Johansson, & Hedenqvist, 2004; Monahan, German, & Kinsella, 1995). Most of the researches in protein based films use this method because it is simple, reproducible in most laboratories and useful as a first approximation to the formation of protein films. However, the drying step makes this method slow and discontinuous, making it infeasible for an industrial scale (Krishna et al., 2012; Reddy & Yang, 2013).

Although thermo-mechanical processing has received less attention, these technologies can use pre-existing equipment for thermoplastics with minimal modifications (Cunningham et al., 2000; Gällstedt et al., 2004; Krishna et al., 2012; Mangavel et al., 2004). Extrusion is a continuous and high performance process, advantageous for industrial scale (Krishna et al., 2012; Reddy & Yang, 2013). On the other hand, compression molding, which is usually assisted by a prior intensive mixing, is generally studied at laboratory scale as a precursor to continuous extrusion with the aim of determining the suitable processing conditions (Hernandez-Izquierdo & Krochta, 2008). During the thermo-mechanical processing, proteins disaggregate, denature and dissociate. These changes result in a complete restructuring of the protein molecules and allow them to recombine, crosslink and aggregate through specific links (Hernandez-Izquierdo & Krochta, 2008; Kuktaite et al., 2011). Particularly, glycinin (11S) has a quaternary structure composed of acidic and basic polypeptides, associated by disulfide bridges. During heat treatment 11S molecules unfold and part of the hydrophobic residues, SH groups and SS bonds are exposed. The

intermolecular polymerization, which in turn leads to protein aggregation, may occur via these groups by the formation of disulfide bridges by oxidation of sulfhydryl groups and the reorganization of intramolecular disulfide bonds to intermolecular disulfide bonds through thiol–disulfide exchange reactions, resulting in an intermolecular network (Gällstedt et al., 2004; Lodha & Netravali, 2005). Parameters such as temperature, pressure, time and plasticizers determine the degree of conformational changes, protein aggregation and chemical crosslinking that take place during processing (Gällstedt et al., 2004; Ullsten et al., 2009). The crosslinking via SH and SS groups is highly dependent on temperature, therefore processing temperature will have significant effects on the final properties of the films (Kim, Weller, Hanna, & Gennadios, 2002; Park, Scott Whiteside, & Cho, 2008; Rhim et al., 2000; Sun, Song, & Zheng, 2008). A greater degree of crosslinking in the network will result in films with higher microstructures density, decreased solubility and improved mechanical strength and barrier properties (Mo & Sun, 2002; Ustunol & Mert, 2004).

The combination of bonds and interactions established between protein chains cause protein based films to be fragile and brittle (Sothornvit & Krochta, 2001). Therefore, is usually necessary to add plasticizers to reduce interactions between protein chains in order to improve their processability and the mechanical properties of the final material. Plasticizers increase chain mobility by reducing interactions between proteins and replacing them with protein–plasticizer interactions (McHugh & Krochta, 1994). Consequently, they increase the flexibility and reduce the brittleness of the films. However, the increased mobility of the chains also causes an increase in the diffusion coefficient of water vapor and oxygen, and as well lowers the mechanical strength of the films. Therefore, the content of plasticizer must be optimized to produce films with desirable mechanical strength, reducing the adverse effect on its properties (Hernandez-Izquierdo & Krochta, 2008; Hettiarachchy & Eswaranandam, 2005). Plasticizers used in biopolymers include polyols, such as sorbitol, glycerol and glucose, among others (McHugh & Krochta, 1994; Rhim et al., 2000; Singh et al., 2008; Sothornvit & Krochta, 2001). Among these plasticizers, glycerol (Gly) is one of the most widely used in protein processing. Soy proteins plasticized with Gly have good processing properties with good final properties (Sothornvit & Krochta, 2001).

The objective of this work was to study the effect of the processing method on the physicochemical, mechanical, and functional barrier of SPC based films. Two methods were used and compared, the traditional method of casting and intensive mixing followed by compression molding. For both methods, the influence of the addition of varying amounts of glycerol on the final properties was also studied.

## 2. Materials and methods

### 2.1. Materials

Soy protein concentrate (SPC, Solcom S 110) with an average particle size of 100 mesh, and proximate composition of 7% moisture, 69% protein, 1% fat, 3% fiber, 5% ash and about 15% non-starch polysaccharides (NSP, mainly cellulose, non cellulose polymers and pectin polysaccharides), was kindly provided by Cordis S.A. (Villa Luzuriaga, Buenos Aires, Argentina). Glycerol analytical grade (Gly, 98%) was purchased from Anedra (Buenos Aires, Argentina) and used as a plasticizer. Sodium hydroxide (NaOH, Anedra) was used to produce pH 10 solution. TRIZMA/hydrochloric acid (Biopack; Buenos Aires, Argentina), glycine (Biopack) Na<sub>2</sub>EDTA (Biopack), sodium dodecyl sulfate (SDS; Anedra), urea (Anedra) and 2-mercaptoethanol (Aldrich, St. Louis, USA) were used for

differential solubility assays. Calcium chloride (CaCl<sub>2</sub>; Aldrich) was used as desiccant for water vapor transmission measurements.

## 2.2. Film preparation

### 2.2.1. Solution casting

SPC was manually mixed with Gly in suitable proportions (30, 40 and 50% w/w SPC dry basis) for 15 min. Afterward, film forming solutions were obtained dissolving the premixes in pH 10 phosphate buffer solution (5 g SPC/100 ml solution; Anedra, Argentina) with constant stirring for 30 min at 70 °C (Cole–Parmer, USA). Finally, the dispersions were treated in an ultrasonic bath (Testlab, 160 W, 40 KHz) for 15 min in order to remove bubbles, and subsequently poured into leveled Teflon-coated Petri dishes. Target film thickness was 150 μm, so the quantity of film forming solution used was calculated so that the solid content was the same (i.e. approximately 35 ml/150 cm<sup>2</sup>, for SPC – 30% Gly). Samples were left to dry in an air-circulating oven at 25 °C (Memmert, Germany), until attaining constant moisture content (approximately 24 h), and then peeled-off from the plates. Films were named C-SPCX, where X corresponds to the weight percentage of plasticizer in the sample.

### 2.2.2. Compression molding

SPC was manually mixed with Gly (30–50% w/w SPC) and pH 10 buffer solution (50% w/w SPC) for 15 min to obtain a workable dough-like material. Afterward the premixes were intensively mixed in a heated roller mixer at 70 °C, 50 RPM for 30 min. Subsequently the mixtures were compression molded by using a hydraulic press (EMS, Buenos Aires, Argentina). Approximately 5 g of mixture were placed between two Teflon sheets of 30 × 30 cm<sup>2</sup>, using a 150 μm frame to regulate the thickness of the films. The system was then placed between two preheated (150 °C) polished stainless steel plates of 30 × 30 × 1 cm<sup>3</sup> and then subject to the following pressing cycle, determined from exploratory studies:

- Stage 1: 150 °C for 5 min at 10 kg cm<sup>-2</sup>,
- Stage 2: 150 °C for 2 min at 100 kg cm<sup>-2</sup>,
- Cooling up to 30 °C, for approximately 30 min.

Films were named M-SPCX, where X corresponds to the weight percentage of Gly in the sample.

## 2.3. Film characterization

### 2.3.1. Preconditioning

Prior testing film samples were preconditioned in laboratory environmental chamber at 25 ± 2 °C and 65 ± 2% RH for 48 h.

### 2.3.2. Thickness

Film thickness (*L*) was measured with a manual micrometer (0–25 ± 0.01 mm, Bta. China). Measurements were done at ten random points along the films. For tensile test, opacity and moisture absorption experiments, four measurements were done on each specimen.

### 2.3.3. Color and light barrier properties

Color parameters were assessed using a portable colorimeter (Lovibond RT 500, United Kingdom) with a measuring area of 8 mm of diameter. Film samples were placed on a white plate, and the Hunter Lab color scale was used: *L*\* = 0 (black) to *L*\* = 100 (white); *a*\* = - 80 (green) to *a*\* = 100 (red); and *b*\* = - 80 (blue) to *b*\* = 70 (yellow). The total color difference ( $\Delta E$ ), was calculated using the following equation:

$$\Delta E = \left[ \left( L_{\text{standar}}^* - L_{\text{sample}}^* \right)^2 + \left( a_{\text{standar}}^* - a_{\text{sample}}^* \right)^2 + \left( b_{\text{standar}}^* - b_{\text{sample}}^* \right)^2 \right]^{0.5} \quad (1)$$

Visible light barrier properties of films were determined by measuring their light absorption at wavelength ranging from 400 to 800 nm, using a UV–Visible spectrophotometer UV–Visible Agilent 8453 (China). Film opacity (*O<sub>p</sub>*) was calculated as the area under the recorded curve and was expressed as absorbance units (AU) × nm. Transparency percentage at a wavelength of 600 nm (*T<sub>600</sub>*) was calculated from the respective absorbance (*A*) by the following equation:

$$A = -\log(T_{600}/100) \quad (2)$$

The results are the average of four readings.

### 2.3.4. Moisture content (MC) and total soluble matter (TSM)

Square-shaped samples (dimensions 4 cm<sup>2</sup>) were weighed using an analytical balance (±0.0001 g; Ohaus, USA) in order to determine the initial mass (*m<sub>i</sub>*). Samples were then dried in an air-circulating oven at 105 ± 1 °C for 24 h (Memmert, Germany). MC was determined as the percentage of mass lost during drying:

$$MC(\%) = (m_i - m_d) \cdot m_i^{-1} \cdot 100 \quad (3)$$

where *m<sub>i</sub>* and *m<sub>d</sub>* are the initial and final mass (dry) of the films, respectively. Three replicates were measured for each composition.

TSM was expressed as the percentage of film dry matter solubilized after 24 h immersion in distilled water. Two methods, proposed by Rhim et al. (1998), were used in order to evaluate the effect of drying the films prior to the determination.

In the first method, *dry method* (TSM<sub>1</sub>), samples were weighed and subsequently dried in an air-circulating oven at 105 ± 1 °C for 24 h to determine their initial dry matter. Afterward, the samples were immersed in 30 mL of distilled water with traces of sodium azide (0.02%) to prevent microbial growth, and stored at 25 ± 2 °C for 24 h. Insoluble dry matter was determined recovering the immersed samples and drying them in an air-circulating oven (Memmert, Germany) at 105 °C for 24 h. Dry soluble matter was calculated subtracting the insoluble dry matter weigh to the initial dry matter.

In the *wet method* (TSM<sub>2</sub>), in contrast, the test samples were not subjected to thermal pretreatment. The samples were weighed and immersed directly in distilled water at 25 ± 2 °C for 24 h. Afterward, the samples were extracted and dried in an oven at 105 ± 1 °C for 24 h to determine dry matter soluble. The necessary initial dry matter values were calculated using MC results. TSM<sub>1</sub> and TSM<sub>2</sub> were calculated as the average of three replicates.

### 2.3.5. Protein solubility

To establish the forces involved in the film stabilization the method proposed by Hager (1984) was used, which consists in dissolving samples in different solutions which are known to disrupt specific protein interactions and bonds. This method was adapted and used by various authors in different protein systems (Guckian, Dwyer, O'Sullivan, O'Riordan, & Monahan, 2006; Jiang, Xiong, Newman, & Rentfrow, 2012; Liu & Hsieh, 2008; Mauri & Añón, 2006; Rhim et al., 2000;). In this work the procedure described elsewhere (Mauri & Añón, 2006) was used, with some modifications. The solutions used were:

- Solution S1: 0.086 M TRIZMA/HCl, 0.09 M glycine and 4 mM Na<sub>2</sub>EDTA;
- Solution S2: S1 + 5 g ml<sup>-1</sup> sodium dodecyl sulfate (SDS);
- Solution S3: S1 + 8 M urea;
- Solution S4: S1 + 5 mg ml<sup>-1</sup> SDS and 8 M urea
- Solution S5: S1 + 5 g ml<sup>-1</sup> SDS, 8 M urea and 25 mg ml<sup>-1</sup> 2-mercaptoethanol (2-ME).

Film samples (approximately 150 mg) were carefully weighted and placed in test tubes with 3 ml of denaturing solution at 20 °C for 24 h. Afterward, suspensions were centrifuged at 9000× *g* for 20 min. Finally the protein content of 1 ml of supernatant was determined with Biuret reagent. In summary, 4 ml of Biuret reagent (1.5 g de CuSO<sub>4</sub>, 6 g de K and Na tartrate tetrahydrate and 8 g of NaOH in 1000 ml of distilled water) and 1 ml of the test solution were mixed and incubated for 5 min at room temperature, and then the absorbance at 530 nm was measured in a UV–Visible spectrophotometer (UV–Visible Agilent 8453, China). Soluble protein content was expressed as the solubilized protein mass of the total protein mass in the film. For each solution (S1 to S5) a calibration curve was performed using human albumin 20% (ZLB Behring), preparing solutions with protein contents from 0 to 10% (w/v).

The procedure used to determine the protein content in solution S5 requires a previous stage of solvent separation, since the 2-ME interferes with the Biuret reagent. The protein dissolved in the supernatant was precipitated by adding 1 ml of trichloroacetic acid (600 g. L<sup>-1</sup>) and centrifuged at 9000× *g* for 20 min. The precipitate was separated and washed twice with 98% ethanol. Finally the precipitate was redissolved with 2 ml of 1 M NaOH prior to the Biuret assay.

### 2.3.6. Attenuated total reflectance – Fourier transformed infrared (ATR-FTIR)

ATR-FTIR spectra were carried out on a Thermo Scientific Nicolet 6700 spectrometer (Wisconsin, USA). The measurements were recorded between 400 and 4000 cm<sup>-1</sup> using an attenuated total reflectance accessory (ATR) with a diamond ATR crystal. A total of 32 scans were performed at 4 cm<sup>-1</sup> resolution. To resolve overlapping peaks and study the secondary structures of proteins the second derivative of the amide I band (1600–1700 cm<sup>-1</sup>) was carried out.

### 2.3.7. Tensile properties

Tensile tests were performed on an INSTRON 4467 Universal Test Machine (Buckinghamshire, England) equipped with a 0.5 KN load cell at a crosshead speed of 3 mm/min at room temperature, according to the procedure described in ASTM D1708-02a. Tensile strength (TS), elongation at break (ε<sub>b</sub>) and elastic modulus (*E*) were calculated as the average of ten replicates.

### 2.3.8. Scanning electron microscopy (SEM)

The films failure surfaces were observed with a Jeol JSM-6460LV (Tokyo, Japan) scanning electron microscope using 10 kV as accelerating voltage. Prior to the observation, the surfaces were sputter-coated with a gold layer of about 100 Å to avoid charging under the electron beam.

### 2.3.9. Barrier properties

Water vapor permeability was measured using the desiccant method, described in ASTM E96-00. Designed capsules were used according to the specifications of this standard. The desiccant (CaCl<sub>2</sub>, PA, Aldrich, St. Louis, USA) was placed in the capsules, covering the whole surface and leaving a gap of 0.5 cm. The films were placed on the capsules, sealing with silicone grease, exposing a film area of 5 cm diameter (*A*). The system was placed in a controlled humidity chamber at 65% RH and 25° C. Mass increase

was determined at specific intervals, until six measurements. The results were plotted as the mass change Δ*m* (g) vs. *t* (h), from whose gradient was obtained the permeation rate of water vapor through the film *G* (g h<sup>-1</sup>). Then, the permeability is obtained as:

$$WVP = G \cdot L \cdot [A \cdot S \cdot (HR_1 - HR_2)]^{-1} \quad \left[ \text{g (Pa h cm)}^{-1} \right] \quad (4)$$

where *L* is the thickness of the film, *S* is the vapor pressure of pure water at the test temperature, and (HR<sub>1</sub>, HR<sub>2</sub>) is the relative humidity gradient used in the assay.

Oxygen permeability coefficient (OPC) determination was carried out using an oxygen permeability analyzer Model 8500 Systech Instruments (Oxon, UK), which operates according to ASTM 3985-02. Samples were cut circumferentially with a diameter of 14 cm and placed in the diffusion chamber of the equipment at 25 °C. The computer monitors the amount of oxygen through the film per unit time and area to reach steady state. The results are reported as the oxygen transfer rate OTR (cm<sup>3</sup> (m<sup>2</sup> day)<sup>-1</sup>). The oxygen permeability coefficient (OPC) can be obtained by the following equation:

$$OPC = (OTR \cdot L) \cdot \Delta P^{-1} \quad \left[ \text{cm}^3 \mu\text{m (m}^2 \text{ day)}^{-1} \right] \quad (5)$$

where *L* is the thickness of the film (μm), Δ*P* is the partial pressure gradient of oxygen through the film (kPa).

### 2.3.10. Statistic analysis

Statistical analysis of results was performed using Origin Pro 8 (Origin Lab Co.). Tukey's test (α = 0.05) was used to detect differences among mean values of film properties.

## 3. Results and discussion

### 3.1. Processing conditions. Preliminary assays

#### 3.1.1. Solution casting

Solution casting requires a first step of dissolution which is usually assisted by temperature in order to promote the disruption of native interactions (Gennadios, Brandenburg, Weller, & Testin, 1993; Monahan et al., 1995). This temperature will strongly depend on the denaturalization temperature of protein fractions. Previously reported calorimetric studies carried out on this commercial SPC showed no transitions associated with the denaturalization of the protein fractions conglycinin and glycinin, associated with the industrial method of obtention (de la Caba et al., 2012; Ciannamea, Martucci, Stefani, & Ruseckaite, 2012). However, some secondary structures remained in the SPC as evidenced by FTIR in a previous work. Thus, dissolution above room temperature would promote the denaturalization of such remaining structures and also would favor the dissolution carbohydrate fraction in SPC (de la Caba et al., 2012). The SPC showed low solubility at room temperature, so the dissolution temperature was rose until the solution was clear. Taking into account that the upper limit of the processing window is given by the evaporation of solvent (100 °C), the temperature for the dissolution step was set at 70 °C. This value agrees with those reported by other authors for SPI (Choi, Kim, Hanna, Weller, & Kerr, 2003; Kokoszka et al., 2010; Rhim et al., 2000; Sun et al., 2009).

In a second step, the film-forming solution is placed in a suitable mold and the solvent is evaporated under controlled conditions. This step was performed at 25 ± 2 °C in an air-circulating oven. Through exploratory studies it was found that at higher temperatures (i.e. 50, 70 °C) drying was excessively fast, causing unwanted shrinkage and cracking of the films. On the other hand, the drying



at room temperature without forced convection was too slow and the colonization by fungi was observed in the samples.

Exploratory studies carried out in this study showed that a minimum concentration of 5% of SPC (w/v) was required to obtain stable and malleable films after drying. It was not possible to obtain stable films with SPC concentrations lower than 5%. Probably, at low SPC concentrations weak cohesive forces resulted in the inability to establish effective protein–protein interactions during drying. On the other hand, if the concentration of SPC was greater than 5% (i.e. 10%), the viscosity of the film-forming solution was excessive (610–628 cp apparent viscosity at a rate of  $2.75 \text{ s}^{-1}$  (Ciannamea et al., 2012)), hindering the proper distribution of the solution in the mold, resulting in uneven thickness.

The formation of protein films is highly dependent on pH (Gennadios et al., 1993; Mauri & Añón, 2006; Monahan et al., 1995). At pH values near the protein isoelectric point (soy protein pI: 4.2–4.6) positive and negative charges are equals, and proteins are coagulated, causing their precipitation. Far from the isoelectric region proteins unfold and denaturalize, exposing reactive polar and no polar groups. Moreover, at alkaline pH disulfide interactions are promoted, since the pK of protein thiols is around pH 8.7–9 (Monahan et al., 1995). From our previous studies it was found that SPC films obtained at pH 10 exhibited a compact structure, while SPC7 film displayed a less ordered arrangement (de la Caba et al., 2012). Moreover, SPC films obtained at pH 7 were less flexible and easy to disintegrate than films formed at pH 10. Therefore a pH 10 buffer solution was used.

Glycerol concentration was varied taking into consideration that the values reported in the literature for SPI films are between 30 and 70% (w/w dry basis SPI) (Choi et al., 2003; Hettiarachchy & Eswaranandam, 2005; Kokoszka et al., 2010; Song et al., 2011). From exploratory studies it was found that Gly concentrations under 30% did not impact significantly in the mechanical properties and the resulting films were brittle. Conversely, films with Gly contents above 50% were unstable, had low mechanical strength and showed evident plasticizer migration to the surface of the film.

### 3.1.2. Compression molding

Thermo-mechanical methods require a previous stage of protein thermo-plasticization in order to obtain mixtures with enough fluidity to be processed. Without added water and/or plasticizers the strong protein–protein intermolecular interactions would lead to thermal degradation of the material before the film can be formed (Hernandez-Izquierdo & Krochta, 2008). Therefore, prior to compression molding, the first step was to perform an intensive mixing under controlled conditions of temperature, speed and time, where through the addition of a suitable combination of water-glycerol a malleable mixture capable to be molded was obtained. Preliminary studies conducted on mixtures of SPC-Gly showed the need to add a combination of water-Gly as plasticizers in order to achieve a workable dough. In general, it was observed that the SPC-Gly mixtures required a minimal Gly and water concentration (30 and 50%, respectively) to achieve sufficient flowability. In agreement with casting conditions pH 10 solution was used (50% w/w SPC) in combination with glycerol to thermo-plasticize the SPC.

Mixing temperature was selected taking into consideration that has to be sufficient to ensure the fluidity of the mixture, but below  $100 \text{ }^\circ\text{C}$ , to prevent water loss at this stage as well as thermo-mechanical degradation of low molar mass fragments of SPC (oligopeptides, oligosaccharides, etc.). Therefore, mixing temperature was set at  $70 \text{ }^\circ\text{C}$  and the speed fixed at 50 rpm. This speed was enough to produce a homogeneous mixing and could be applied for a maximum time of 30 min without producing evident degradation. Experimentally it was found that at higher temperatures (i.e.:

80,  $90 \text{ }^\circ\text{C}$ ) or mixing speeds higher than 50 RPM, the produced mixtures had an intense yellow–brown coloration, due to protein degradation in addition to the degradation of the carbohydrate fraction of the SPC (Hernandez-Izquierdo & Krochta, 2008; Krishna et al., 2012; Martucci & Ruseckaite, 2009).

Molding temperature and time were established from exploratory studies. The lower limit of the processing window is given by the temperature required to achieve protein denaturalization ( $79$  and  $95 \text{ }^\circ\text{C}$  for 7S and 11S fractions). According to several authors, processing temperatures higher than  $100 \text{ }^\circ\text{C}$  promotes greater soy protein denaturalization and greater protein crosslinking (Cunningham et al., 2000; Hernandez-Izquierdo & Krochta, 2008; Sothornvit, Olsen, McHugh, & Krochta, 2003). However, too high temperatures can cause protein degradation and the disruption of disulfide bonds, which impose the upper limit of the processing window (Gällstedt et al., 2004; Ogale, Cunningham, Dawson, & Acton, 2000; Ullsten et al., 2009). For example, Cunningham et al. (2000) obtained SPI-Gly films by compression molding at  $150 \text{ }^\circ\text{C}$ , 10 MPa, and 2 min while Paetau et al. (1994) indicated an optimum molding temperature of  $140 \text{ }^\circ\text{C}$ . Through preliminary studies it was determined that a minimum molding temperature of  $110 \text{ }^\circ\text{C}$  was needed, since below this temperature the films had a dough aspect, being opaque and whitish and broke when they were detached from the mold, presumably due to a low degree of crosslinking (Gällstedt et al., 2004). The upper limit of the processing window was set at  $170 \text{ }^\circ\text{C}$  to avoid protein degradation, taking into account previous thermogravimetric analysis (Ciannamea et al., 2012). In order to select the optimum molding temperature, SPC films plasticized with 30% Gly were obtained at temperatures between  $110$  and  $170 \text{ }^\circ\text{C}$  and pressing times of 1–9 min. Heat induces the formation of covalent interactions (SS), which leads to a reduction in solubility of the films (Hernandez-Izquierdo & Krochta, 2008; Rhim et al., 2000). The effect of the cross-linking induced by heat could be observed by a gradual decrease in the water solubility of the films with increasing processing temperature from  $110$ – $150 \text{ }^\circ\text{C}$ . Films processed at  $160$  and  $170 \text{ }^\circ\text{C}$  showed a brownish color, probably due to degradation of the protein and/or carbohydrates present in SPC, so it could be inferred that such temperatures were excessive for film processing. Films processed at  $150 \text{ }^\circ\text{C}$  and 5 min showed the lowest solubility, indicating higher crosslinking. Therefore these conditions were selected as optimal for compression molding.

### 3.2. Visual aspect, light barrier properties and color

Transparent and flexible SPC based films with 30–50% of Gly were obtained. Particularly, plasticized M-SPC films had smooth surfaces and were visually homogeneous, transparent and slightly yellowish (Fig. 1). C-SPC films were visually similar, except they were more opaque, had rougher surfaces and in some cases display bubbles, despite the ultrasonic bath treatment of film forming solutions. No significant differences ( $p > 0.05$ ) in average thickness values were detected irrespective of the processing method or Gly concentrations (Table 1). Uniformity in this parameter should be taken into account when calculating opacity, some tensile properties as well as barrier properties, which are thickness dependent properties (McHugh, Avena-Bustillos, & Krochta, 1993).

Confirming visual observations, irrespective the concentration of Gly, M-SPC films showed higher transparency values (lower opacity) than C-SPC films ( $p < 0.05$ ), reaching  $T_{600}$  of an order of magnitude higher than casting films (Table 1). For example, the  $O_p$  and  $T_{600}$  of M-SPC30 films were  $668 \pm 4 \text{ AU nm}$  and 2.3%, respectively, and  $955 \pm 10 \text{ UA nm}$  and 0.47% for C-SPC30 films. Park et al. (2008) reported that compression molding processing produced gelatin films with smoother surfaces, conferring greater transparency.

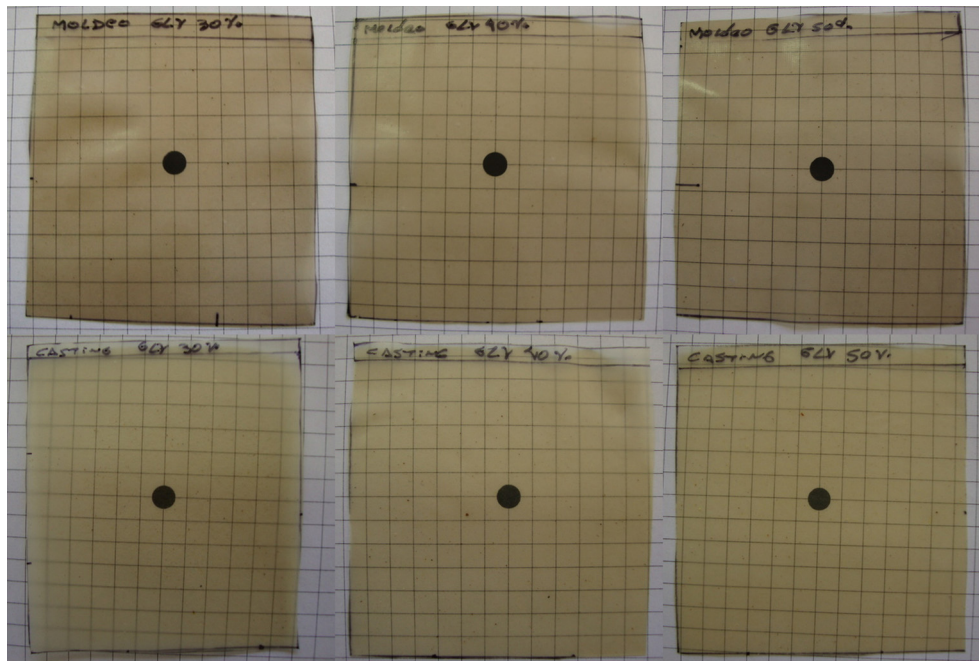


Fig. 1. Photographs of SPC films obtained by compression molding (above) and casting (below), with concentrations of Gly 30% (left) to 50% (right).

Generally, the incorporation of Gly promotes more transparent films since the plasticizer interferes with the interactions between protein chains, decreasing the absorbance in the visible region (Sothornvit & Krochta, 2001). M-SPC50 films had lower  $O_p$  compared to M-SPC30 films (Table 1,  $p < 0.05$ ). However, in C-SPC films the addition of 50% Gly resulted in more opaque films (with the concomitant decrease in transparency) ( $p < 0.05$ ). This fact may be related to the presence of Gly-rich and protein-rich domains, as reported by Chen and Zhang (2005). Authors showed that this micro-phase separation takes place in SPI-Gly films under Gly concentrations above of 25% (w/w) and that the size of Gly-rich domains increases with its concentration (Chen & Zhang, 2005). From these results it can be postulated that at certain Gly level higher than a critical volume fraction, the plasticizing effect is counterbalance by the phase segregation process induced by the limited compatibility between the plasticizer and the matrix. The dispersed phase having a different refractive index than the gelled matrix might lead to decreased film transparency due to light scattering.

Color parameters showed no significant differences with plasticizer concentration, regardless the processing method ( $p > 0.05$ , Table 1). Furthermore,  $b^*$  values of M-SPC and C-SPC films were similar and close to 13, which is related to the characteristic yellowish of soy protein based films (Denavi et al., 2009; Kim et al., 2002; Kunte et al., 1997; Rhim et al., 2000). This result is an interesting fact since it has been reported for several proteins including soybean (Garrido, Etxabide, Peñalba, de la Caba, & Guerrero, 2013)

and whey (Sothornvit et al., 2003) that dry methods produce films with greater coloration (higher  $b^*$ ) than those obtained by casting, due to shear or thermal degradation.

### 3.3. Interactions involved in the film formation

In order to get a better insight on structural characteristics of SPC films obtained by both processing methods, film samples were analyzed by ATR-FTIR. Spectra of SPC-Gly films at two different glycerol levels (Fig. 2) were similar to previous reports (Chen & Subirade, 2009; Ciannamea, Sagüés, Saumell, Stefani, & Ruseckaite, 2013), showing peaks of relevance at 1630, 1530, 1230  $\text{cm}^{-1}$ , characteristic of amide I (C=O stretching), amide II (N-H bending) and amide III (C-N and N-H stretching), respectively (Chen & Subirade, 2009). The peaks at 850  $\text{cm}^{-1}$ , 900  $\text{cm}^{-1}$ , 925  $\text{cm}^{-1}$  (C-C vibrations), 1045  $\text{cm}^{-1}$  (C-O stretching at C1 and C3), and 1117  $\text{cm}^{-1}$  (C-O stretching at C2) were ascribed to Gly (Lodha & Netravali, 2005), whereas the broad adsorption band between 3500 and 3200  $\text{cm}^{-1}$  was attributed to free and bound OH groups in SPC and Gly. The addition of Gly induced a slight reduction in the intensity of the amide II band, which is generally related with changes in hydrogen bonding because of the medium, confirming that Gly acts by interacting with protein chains and reducing the bindings between the chains. This leads to a less dense and more disorganized polymeric matrix in the presence of Gly (Sothornvit & Krochta, 2001).

Table 1  
Thickness and optical properties of SPC films.

	$L$ ( $\mu\text{m}$ )	$O_p$ (AU. nm)	$T_{600}$ (%)	$L^*$	$a^*$	$b^*$	$\Delta E$
C-SPC30	143 $\pm$ 22 a	955 $\pm$ 10 a	0.47 $\pm$ 0.03 a	82.9 $\pm$ 1.4 a	0.8 $\pm$ 0.2 a	12.6 $\pm$ 2.6 a	21.3 $\pm$ 2.9 a
C-SPC40	153 $\pm$ 33 a	968 $\pm$ 24 a	0.43 $\pm$ 0.05 a	82.5 $\pm$ 1.9 a	0.9 $\pm$ 0.3 a	12.7 $\pm$ 3.7 a	21.5 $\pm$ 4.2 a
C-SPC50	155 $\pm$ 19 a	1001 $\pm$ 16 b	0.35 $\pm$ 0.03 b	82.2 $\pm$ 1.6 a	0.9 $\pm$ 0.3 a	13.4 $\pm$ 2.8 a	22.3 $\pm$ 3.2 a
M-SPC30	139 $\pm$ 14 a	668 $\pm$ 4 c	2.3 $\pm$ 0.0 c	75.3 $\pm$ 1.4 b	2.5 $\pm$ 0.2 b	12.8 $\pm$ 1.5 a	25.4 $\pm$ 2.1 a
M-SPC40	135 $\pm$ 14 a	618 $\pm$ 7 d	3.2 $\pm$ 0.1 d	76.8 $\pm$ 0.8 b	2.3 $\pm$ 0.2 b	13.4 $\pm$ 1.3 a	24.9 $\pm$ 1.5 a
M-SPC50	148 $\pm$ 10 a	580 $\pm$ 18 e	3.9 $\pm$ 0.4 e	75.3 $\pm$ 0.8 b	2.4 $\pm$ 0.3 b	13.6 $\pm$ 0.6 a	26.0 $\pm$ 0.9 a

Mean values  $\pm$  standard deviations. Mean values within the same column followed by the same letter are not significantly different ( $p > 0.05$ , Tukey test).

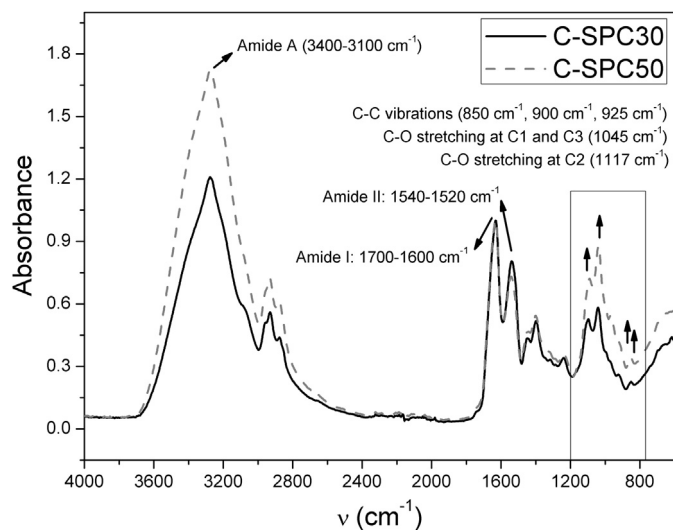


Fig. 2. ATR-FTIR spectra of C-SPC30 and C-SPC50 films.

Fig. 3a shows the spectra of SPC30 obtained by both processing methods. The amide I band is the most often used to study in depth changes in the protein secondary structure (Barth, 2007). Therefore, the detailed analysis of this region facilitates the

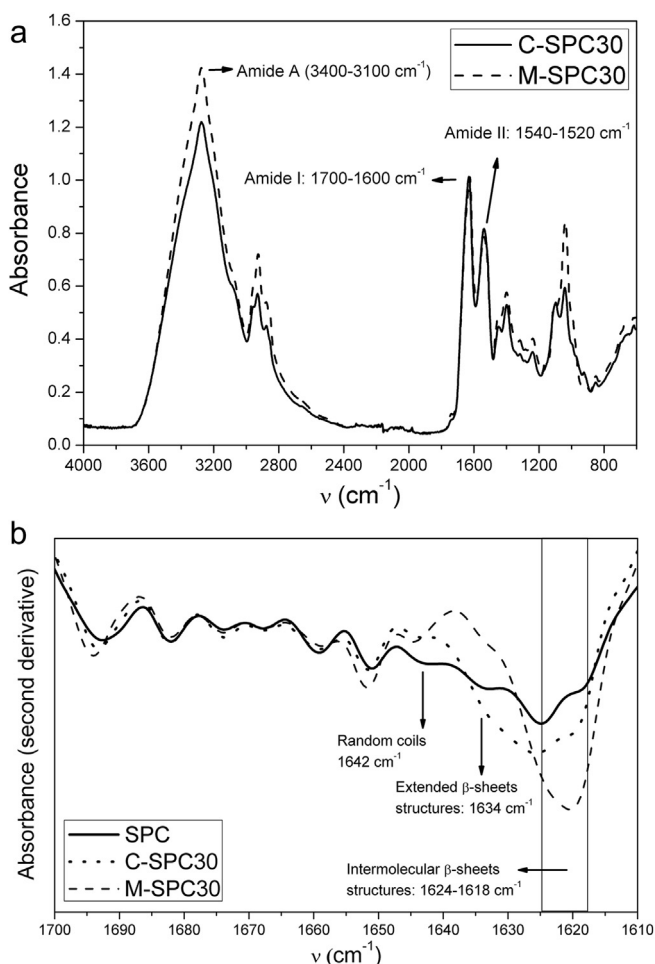


Fig. 3. a) ATR-FTIR spectra of C-SPC30 and M-SPC30 films. b) Amide I Band: Second derivative of ATR-FTIR spectrum of commercial SPC, C-SPC30 and M-SPC30 films.

understanding of the conformational changes due to the plasticizer and the processing methods. To improve the spectral resolution and identify the main components that make up the amide I band of SPC-Gly films, the second derivative was applied and the spectrum is displayed in Fig. 3b. Compared with unprocessed SPC powder, films obtained by casting showed a reduction in the intensity of the band at  $1642\text{ cm}^{-1}$ , which is associated with disordered structures (random coils) and a sharp increase in the intensity of the bands in the region  $1634\text{--}1618\text{ cm}^{-1}$ , related with  $\beta$ -sheet structures, both extended and intermolecular type (Kuktaite et al., 2011; Ullsten et al., 2009). These results suggest a conformational change from a structure with a high contribution of random coils to a structure with a greater amount of  $\beta$ -sheet structures (Kuktaite et al., 2011; Ullsten et al., 2009). This observation was even more distinctive in the films processed by compression molding. M-SPC films, compared with SPC powder, showed not only a lower intensity of the band at  $1642\text{ cm}^{-1}$ , but also a reduction in the intensity of the band at  $1634\text{ cm}^{-1}$ , associated with extended  $\beta$ -sheet structures. Moreover, there was a marked increase in the intensity of the bands in the region  $1624\text{--}1618\text{ cm}^{-1}$ , indicating a higher contribution of intermolecular  $\beta$ -sheet structures, which in turn is indicative of a more aggregated structure, greater than in the films obtained by casting (Lefèvre, Subirade, & Pézolet, 2005). It has been reported that the formation of intermolecular disulfide bridges play an important role in protein aggregation (Lefèvre et al., 2005). Temperature has a strong influence in promoting the exposure of functional and hydrophobic groups and facilitating the formation of covalent interactions (disulfide bridges), consequently increasing the degree of protein aggregation (Hernandez-Izquierdo & Krochta, 2008).

Physical and chemical interactions that take place during the film formation have a great impact on the final properties and microstructure. The possible contribution of hydrogen-bonding interactions is difficult to establish by ATR-FTIR, given the absence of significant down-shifts in the frequency of occurrence of the different band centers. In order to establish the forces involved in the stabilization of films the protein solubility was measured in different specific denaturing buffer solutions, each able to disrupt specific interactions and bond. In this study five denaturing solutions were used with specific action in the protein structure. S1 solution contains TRIZMA/HCl, glycine and EDTA and affects protein electrostatic interactions. S2 (S1 + SDS) can also break hydrophobic interactions, while solution S3 (S1 + UREA) can disrupt hydrogen bonds and small aggregates stabilized by this kind of interaction. S4 solution (S1 + SDS + UREA) breaks all the aforementioned interactions and S5 (S4 + mercaptoethanol) also breaks disulfide bridges (Hager, 1984; Jiang et al., 2012; Liu & Hsieh, 2008; Mauri & Añón, 2006; Rhim et al., 2000;).

Fig. 4 shows the solubility of C-SPC and M-SPC films in these denaturing buffer solutions. The films obtained by casting presented protein solubility in solution S1 of around  $340\text{ }\mu\text{g}\cdot\text{g}^{-1}$ , while the solubility of films processed by compression molding was lower ( $220\text{ }\mu\text{g}\cdot\text{g}^{-1}$ , Fig. 4). This result suggests that electrostatic forces have a minor role in the stabilization of protein networks, and their contribution is lower in thermomechanically processed films (Guckian et al., 2006). The function of SDS in S2 solution is to disrupt non-covalent interactions (electrostatic and hydrophobic). The solubility of C-SPC30 films in S2 buffer increased in approximately 13%, with respect to the S1 buffer. For M-SPC films solubility increased only 6%. This result indicates that hydrophobic interactions were more important in the formation of C-SPC than M-SPC films (Guckian et al., 2006; Mauri & Añón, 2006). In S3 buffer, C-SPC30 films showed a solubility of about  $600\text{ }\mu\text{g}\cdot\text{g}^{-1}$ , being the maximum value observed for casting films, and no significant differences were observed with the addition of 2-ME in the solution



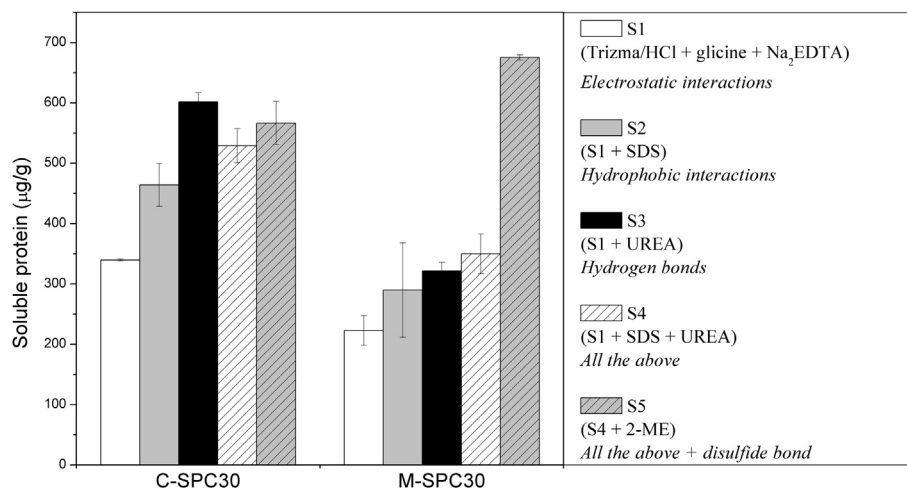


**Fig. 4.** SPC-30 film solubility in different denaturing solutions: S1: 0.086 M TRIZMA/HCl, 0.09 M glycine and 4 mM Na<sub>2</sub>EDTA; S2: S1 + 5 g ml<sup>-1</sup> sodium dodecyl sulfate (SDS); S3: S1 + 8 M urea; S4: S1 + 5 mg ml<sup>-1</sup> SDS and 8 M urea; S5: S1 + 5 g ml<sup>-1</sup> SDS, 8 M urea and 25 mg ml<sup>-1</sup> 2-mercaptoethanol (2-ME).

S5 (able to break disulfide bonds). Apparently, the presence of urea determines the solubility of casting films. These results gave experimental support to the fact that non-covalent interactions (electrostatic, hydrophobic and hydrogen bonding) predominate in the stabilization of the films obtained by casting (Guckian et al., 2006; Jiang et al., 2012; Mauri & Añón, 2006).

By contrast, M-SPC30 films showed lower solubility in solutions S3 and S4 (320–350 µg g<sup>-1</sup>) and no significant differences ( $p > 0.05$ ) in the protein solubility where observed between S2, S3 y S4 solutions. Therefore, in compression molding films a maximum of 35% of the total protein was dissolved disrupting only non-covalent interactions. The marked increase in solubility observed in the presence of S5 buffer, up to 675 µg.g<sup>-1</sup>, implies that disulfide bonding plays an important role in the formation of such films, in agreement with previous results (Guckian et al., 2006; Hager, 1984; Jiang et al., 2012; Mauri & Añón, 2006; Rhim et al., 2000). This result could be associated with the high degree of aggregation observed by ATR-FTIR (Fig. 3b). Consequently, it is possible to assert that the stabilization of SPC films obtained by compression molding is dominated by S–S covalent interactions. This finding agrees well with those previously reported for SPC, SPI-gluten-starch mixtures and wheat gluten films processed by extrusion (Hager, 1984; Liu & Hsieh, 2008; Mangavel et al., 2004). The heat treatment during compression can promote the cross-linking between proteins through intermolecular disulphide bridges, either from free sulfhydryl groups or through thiol–disulfide exchange reactions (Hernandez-Izquierdo & Krochta, 2008; Rhim et al., 2000). In the literature it has been reported that the cross-linking degree of the network and the level of protein aggregation determine the final properties of the films. In particular, it has been reported that a higher crosslinking degree outcome in films with higher microstructure density, lower solubility and improved mechanical

strength and barrier properties (Lefèvre et al., 2005; Mauri & Añón, 2006; Mo & Sun, 2002; Rhim et al., 2000; Sun et al., 2008; Ustunol & Mert, 2004).

### 3.4. Moisture content and total soluble matter

Total soluble matter of films (TSM, Table 2) showed a slight increase with the incorporation of Gly as reported by others (Moore, Martelli, Gandolfo, Sobral, & Laurindo, 2006; Sothornvit et al., 2003); however these differences were not statistically significant ( $p > 0.05$ ). Compression molding films showed lower TSM percentages than those measured on the films obtained by casting (Table 2). It was previously reported that an increase in cross-linking in soybean protein based films provoked a decrease in the solubility of the produced film (Rhim et al., 2000). In the case of M-SPC films this result can be associated with the higher contribution of stabilizing S–S covalent bonds (Gällstedt et al., 2004; Mangavel et al., 2004). The lower solubility of M-SPC films put forward that cross-linking through disulfide bridges takes place during thermal processing, according to the ATR-FTIR and differential solubility studies.

The difference between the TSM<sub>1</sub> (with pre-drying) and TSM<sub>2</sub> (without pre-drying) methods was not significant for M-SPC films ( $p > 0.05$ ), so it can be inferred that the drying step at 105 °C applied to these samples prior to the TSM determination did not significantly modify the stabilizing interactions of the films. Contrary, in films processed by casting, TSM<sub>1</sub> percentages were significantly lower than those of TSM<sub>2</sub> ( $p < 0.05$ ). This result suggests that in these films, where the stabilization is dominated by non-covalent interactions (Fig. 4), the reduced solubility arose through the formation of new S–S bonds during drying at 105 °C. Similar results were observed in SPI-Gly films obtained by casting

**Table 2**  
Moisture content (MC), total soluble matter (TSM) and tensile mechanical properties of SPC-Gly films processed by casting and compression molding.

	MC (%)	TSM <sub>1</sub> (%)	TSM <sub>2</sub> (%)	TS (MPa)	ε <sub>R</sub> (%)	E (MPa)
C-SPC30	17.7 ± 0.7 a	34.7 ± 2.7 a	52.8 ± 3.1 a	2.27 ± 0.20 ab	14.5 ± 2.2 a	48.1 ± 7.3 a
C-SPC40	20.4 ± 0.7 b	36.7 ± 2.8 a	46.7 ± 3.2 b	2.12 ± 0.47 ac	15.8 ± 2.9 a	38.7 ± 8.3 b
C-SPC50	23.6 ± 1.2 c	39.6 ± 4.2 a	45.3 ± 0.9 b	1.73 ± 0.37 c	18.0 ± 1.6 a	32.2 ± 9.2 bc
M-SPC30	21.3 ± 0.8 b	26.3 ± 0.4 b	29.9 ± 0.2 c	3.54 ± 0.18 d	28.0 ± 1.7 b	56.6 ± 7.5 a
M-SPC40	28.1 ± 0.4 d	26.8 ± 0.2 b	30.1 ± 0.3 c	2.63 ± 0.30 b	29.8 ± 3.6 b	26.5 ± 2.2 c
M-SPC50	32.4 ± 0.4 e	27.1 ± 0.3 b	30.9 ± 0.3 c	1.91 ± 0.14 ac	23.6 ± 4.4 c	18.7 ± 1.8 d

Mean values ± standard deviations. Mean values within the same column followed by the same letter are not significantly different ( $p > 0.05$ , Tukey test).



(Rhim et al., 1998) and heat press gelatin-Gly-dialdehyde starch films (Martucci & Ruseckaite, 2009).

Total moisture content of films (MC, Table 2) increased with the amount of Gly, in accordance with the hygroscopic nature of the plasticizer which promotes the moisture retention capacity of the films (Kokoszka et al., 2010; Sothornvit et al., 2003). Increasing the concentration of Gly increases the amount of additional hydroxyl groups in the matrix, which can associate with water enhancing moisture absorption (Kokoszka et al., 2010; Martucci & Ruseckaite, 2009). Similar results have been observed in SPI-Gly obtained by casting (Choi et al., 2003; Kokoszka et al., 2010).

M-SPC films showed significantly higher MC than C-SPC films ( $p < 0.05$ , Table 2). For example, M-SPC50 and C-SPC50 films showed mean moisture contents of 32.4% and 23.6%, respectively. Similar behavior was observed in gelatin-Gly (Krishna et al., 2012) and gelatin-Gly-sorbitol films obtained by extrusion and casting (Park et al., 2008). It is postulated that the largest number of covalent S–S bonds stabilizing M-SPC films impose conformational restrictions, leaving a greater number of hydrophilic polar groups exposed able to bind water molecules, thereby increasing the moisture level of these films.

### 3.5. Tensile properties

Tensile properties determine the mechanical response and the potential applications of the produced films. Fig. 5 shows representative stress–strain curves for films obtained by the two processing methods. These curves exhibit a typical behavior: at low strain (i.e. less than 5% for M-SPC films), tension increases rapidly with the increase in deformation and the slope is within the elastic region, defining the elastic modulus. For greater deformations values, the stress increases more slowly until failure occurs. At first glance, the curves suggest that solution casting produces films with lower deformation than compression molding. The mechanical parameters obtained from these curves are summarized in Table 2 and show this tendency.

M-SPC films exhibited significantly higher TS values than C-SPC films ( $p < 0.05$ ). For example, the TS of M-SPC30 and C-SPC30 films were  $3.54 \pm 0.18$  MPa and  $2.27 \pm 0.20$  MPa, respectively. This behavior may be associated with the disulfide cross-linking and the major aggregation in compression molding films, as observed by differential solubility and ATR-FTIR studies. Films obtained by

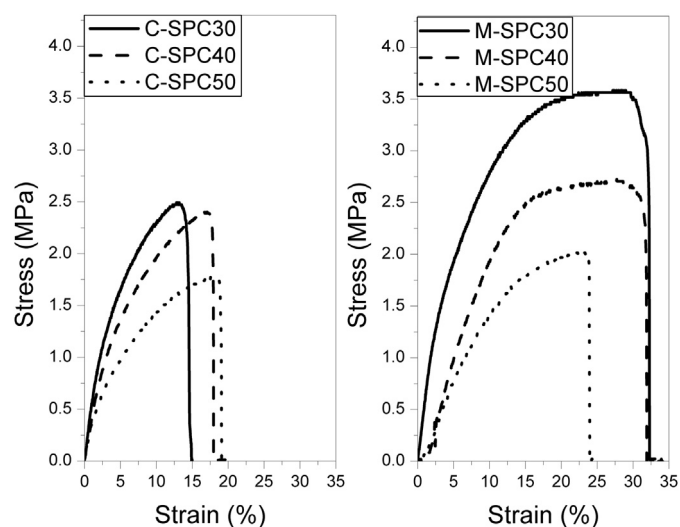


Fig. 5. Stress-strain curves of plasticized films containing 30, 40 and 50% Gly, processed by casting and compression molding.

casting had higher Young modulus ( $E$ ;  $p < 0.05$ ), except for the formulation with 30% Gly, where no significant differences were detected ( $p > 0.05$ ). Sothornvit, Olsen, McHugh, and Krochta (2007) reported  $E$  values of compression molded whey protein films plasticized with 40–50% Gly similar to  $E$  of casting whey protein – 45% Gly films. However this trend seems to disagree with the largest percentage of S–S bonds and the presence of aggregates in the films produced by compression molding. Discrepancies can be ascribed to the plasticizing action of water, the most effective plasticizer for proteins (Hernandez-Izquierdo & Krochta, 2008). Films produced by compression had significantly higher equilibrium MC values ( $p < 0.05$ , Table 2). It is therefore expected that the elastic modulus was reduced by the combined action of Gly and absorbed water (Paetau et al., 1994; Park et al., 2008). The elongation at break was higher ( $p < 0.05$ ) for M-SPC films (i.e.  $28.0 \pm 1.7\%$  for M-SPC30 film and  $14.5 \pm 2.2\%$  for C-SPC30). This result could also be related to the higher moisture content of M-SPC films. Similar trends have been reported for gelatin (Krishna et al., 2012) and whey protein films (Sothornvit et al., 2007).

Irrespectively the processing method, Gly incorporation significantly reduced  $E$  and TS values of the produced films ( $p < 0.05$ ). The elongation at break of C-SPC was not significantly affected ( $p > 0.05$ ) by the Gly level, whereas it was detrimental for M-SPC50 film ( $p < 0.05$ ). This was consistent with the migration of the plasticizer to the film surface due to the reduced free volume because of the increased cross-linking density developed by disulfide bonds in M-SCP films. Similar trend was reported by other thermo-molded protein based films including unaged SPI-Gly films produced by thermal compression (Cunningham et al., 2000), wheat gluten plasticized with Gly (Mangavel et al., 2004) and SPI-Gly films processed by compression molding (Guerrero et al., 2010).

Cross-section of C-SPC and M-SPC films were examined by SEM to obtain some information about their microstructures (Fig. 6). Thermo-pressed films exhibited homogeneous and compact structures compatible with the brittle fracture observed. The analysis also revealed no differences between the microstructure of the films incorporated with different Gly level (Fig. 6a–c). The presence of pores was detected but this feature was minor. The microstructures observed for M-SPC films were comparable to those reported for other thermo-mechanically processed protein films, such as SPI-Gly (Ogale et al., 2000), wheat gluten-Gly (Mangavel et al., 2004). Conversely, C-SPC30 films also revealed compact and homogeneous structures, but exhibited greater porosity than M-SPC30 films (Fig. 6d–f). This could be a consequence of the evaporation process during the drying step of solution casting. Similar microstructures were already reported by other authors in SPI-Gly films obtained by solution casting (Denavi et al., 2009; Sun et al., 2009). Higher concentrations of Gly (40 and 50%) resulted in rougher and less compact surfaces (Ogale et al., 2000). SEM observations suggest that processing method have an important role in the organization of the network at the microscale which in turn determines the properties of the films.

### 3.6. Barrier properties

One of the main functions of food packaging films is to control mass transfer between the food and the environment. Therefore, it is crucial to determine the barrier activity of the films. The water vapor permeability (WVP) indicates the amount of water permeating per unit area and time through the packaging material (Janjarasskul & Krochta, 2010). This property is of great importance in order to extend the food shelf life, where physicochemical and microbiological deterioration is closely related to the water activity. WVP values obtained in this study ranged between  $1.60 \pm 0.04$  and  $6.31 \pm 1.03 \times 10^{-13}$  ( $\text{Kg m}^{-2} \text{s}^{-1} \text{Pa}^{-1}$ )

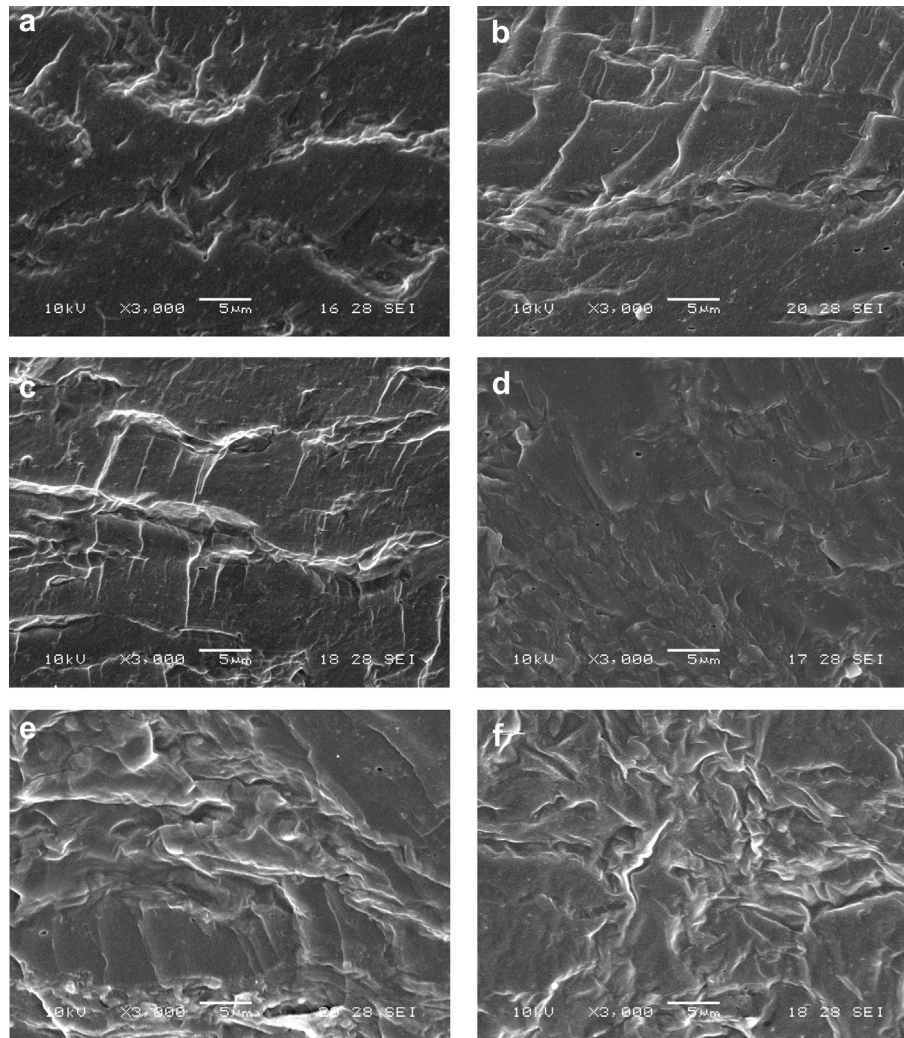


**Fig. 6.** SEM micrographs of the fracture surface of films at 3000x: a) M-SPC30 b) M-SPC40 c) M-SPC50; d) C-SPC30 e) C-SPC40 f) C-SPC50.

and significant differences ( $p < 0.05$ ) were detected between processing methods (Table 3). WVP values of M-SPC films were significantly lower than those observed in C-SPC films ( $p < 0.05$ ). The lower WVP values of M-SPC films compared to cast films could be explained by the compact structure with low pores content associated with a greater presence of S–S bridges due to thermal processing. It is interesting to note the low standard deviation of M-SPC samples, contrary to what observed for solution casting. This result confirms that the entrapped bubbles, pores or cavities evidenced by SEM in C-SPC films (Fig. 6d–f) contribute negatively to WVP.

**Table 3**

Water vapor and oxygen permeability of SPC-Gly films obtained by casting and compression molding.

Gly (%)	WVP $10^{13}$ (Kg m/m <sup>2</sup> s Pa)	OPC (cm <sup>3</sup> µm)/(m <sup>2</sup> día KPa)
C-SPC30	3.09 ± 0.30 ab	8.5 ± 0.8 a
C-SPC40	4.85 ± 0.83 cd	18.5 ± 2.4 b
C-SPC50	6.31 ± 1.03 d	–
M-SPC30	1.60 ± 0.04 ab	15.2 ± 2.0 b
M-SPC40	2.99 ± 0.07 b	27.1 ± 0.0 c
M-SPC50	4.02 ± 0.1 bc	47.4 ± 1.4 d

Mean values ± standard deviations. Mean values within the same column followed by the same letter are not significantly different ( $p > 0.05$ , Tukey test).

The amount of Gly incorporated significantly ( $p < 0.05$ ) affected WVP, irrespective of the processing method; the higher the glycerol content the higher WVP (Table 3). Hydrophilic edible films are very prone to plasticization from water, which tends to cluster within the polymer matrix. It is recognized that an increase in plasticizer is directly proportional to an increase in water vapor permeability (Kokoszka et al., 2010; Krishna et al., 2012; McHugh et al., 1993). Plasticizers modify the molecular organization of the protein network and increase the free volume resulting in less dense network that results in films more permeable to water. For the same reason the OPC values of films containing high Gly level were significantly higher ( $p < 0.05$ ), irrespective of the film forming procedure (Table 3). Thermo-pressed films displayed significantly higher ( $p < 0.05$ ) OPC values than those recorded for casting films at the same Gly level (Table 3). This result was somehow expected and it can be attributed to the higher solubility of O<sub>2</sub> in M-SPC films due to the higher MC registered (Table 2) (Hong & Krochta, 2003). However, for high Gly content in C-SPC films, the SEM micrographs revealed multiple small cracks in the film structure, which play a major role in increasing OPC. In particular, C-SPC50 film was unable to be evaluated since pores present in the microstructure induced holes and cracks during the test favored by the flow of oxygen.

WVP and OPC values of several alternative protein-based films are summarized in Table 4. WVP and OPC values of various

**Table 4**

Comparison of water vapor and oxygen permeability of films based on proteins and synthetic polymers.

	Test conditions (T,RH)		WVP 10 <sup>13</sup> (Kg m/m <sup>2</sup> s Pa)	Test conditions (T,RH)		OPC (cm <sup>3</sup> μm/(m <sup>2</sup> day KPa))
Casting SPI-25% Gly	28 °C	0–78%	4.51 (Stuchell & Krochta, 1995)	–	–	–
Casting SPI-50% Gly	20 °C	0–80%	2.28–3.42 (Jiang, et al., 2012)	25 °C	60%	18.2 (Denavi et al., 2009)
Casting WG-30% Gly	–	–	–	30 °C	0%	17.0 (Park & Chinnan, 1995)
Casting WG-40% Gly	26 °C	50–100%	12.5 (Aydt et al., 1991)	–	–	–
Casting GE-20% Gly	25 °C	50–100%	14.2 (Park et al., 2008)	–	–	–
Casting WPI-30% Gly	25 °C	0–100%	9.2 (Sothornvit et al., 2003)	–	–	–
Compression WG-25% Gly	37.8 °C	49%	2.2–2.3 (Gällstedt et al., 2004)	23 °C	90–95%	22–30 (Gällstedt et al., 2004)
Compression WG-40% Gly	37.8 °C	49%	5.6–6.9 (Gällstedt et al., 2004)	23 °C	90–95%	125 (Gällstedt et al., 2004)
Compression GE-20% Gly	25 °C	50–100%	6.7 (Park et al., 2008)	–	–	–
Compression WPI-30% Gly	25 °C	0–100%	44 (Sothornvit et al., 2003)	–	–	–
HDPE	38 °C	0–90%	0.003 (Delassus, 1997)	20 °C	75%	390–780 (Delassus, 1997)
LDPE	38 °C	0–90%	0.011 (Delassus, 1997)	20 °C	75%	970–1400 (Delassus, 1997)
Nylon-6	38 °C	0–90%	0.081 (Delassus, 1997)	20 °C	75%	7.8–11.6 (Delassus, 1997)
PET	38 °C	0–90%	0.014 (Delassus, 1997)	20 °C	75%	12–16 (Delassus, 1997)
PP	38 °C	0–90%	0.005 (Delassus, 1997)	20 °C	75%	580–970 (Delassus, 1997)
PS	38 °C	0–90%	0.005 (Delassus, 1997)	20 °C	75%	970–1600 (Delassus, 1997)

WPI, whey protein isolate; WG, wheat gluten; GE, gelatin; HDPE, high density polyethylene; LDPE, low density polyethylene; PET, polyethylene terephthalate; PP, polypropylene; PS, polystyrene.

synthetic polymers traditionally used in food packaging films are well documented in the literature and also included for comparison. Results from the present study indicate that SPC-Gly films had WVP values comparable with those reported for wheat gluten (Aydt, Weller, & Testin, 1991; Gällstedt et al., 2004), gelatin (Park et al., 2008) and whey protein (Sothornvit et al., 2003). SPC-Gly films had slightly higher water permeability than reported for SPI-Gly films at the same Gly level (Jiang et al., 2012; Stuchell & Krochta, 1995). The higher WVP of SPC films, compared to those based on SPI, could be explained by the high carbohydrate content in the SPC (about 15%), which confers higher hygroscopic character to the resultant films (Paetau et al., 1994; Stuchell & Krochta, 1995). However, WVP of SPC-Gly films was still higher than those of synthetic polymers (Delassus, 1997). Protein films are usually poor water vapor barriers due to the inherent high hydrophilicity of proteins and the hydrophilic plasticizers added (Kunte et al., 1997). Similarly, OPC values of SPC films were comparable to the previously reported for SPI and other alternative protein films (Denavi et al., 2009; Gällstedt et al., 2004; Park & Chinnan, 1995). SPC-Gly films obtained herein had superior oxygen barrier properties (irrespective of the forming process) than several synthetic plastic films (i.e. low and high density polyethylene, polypropylene, polystyrene (Delassus, 1997)). Protein films are expected to be excellent oxygen barriers since their tightly packed, ordered hydrogen bonded network structure (McHugh & Krochta, 1994). The very good oxygen barrier properties of SPC-Gly films suggest the potential of these films to control oxygen transfer and protect food from degradative oxidation and respiration reactions, in order to improve food quality and extend shelf life.

#### 4. Conclusions

Soybean protein concentrate films can be easily prepared using thermo-compression technique. During thermo-molding unfolding of the remaining secondary structures of soybean proteins facilitates the cross-linking through non covalent and disulfide bonding which significantly influences film properties. In relative terms, M-SCP30 exhibited the most attractive combination of properties for further development toward packaging applications. M-SPC30 films were fivefold more transparent, 25% less soluble, 50% better water vapor barrier, 56% mechanically more resistant and 93% more stretchable due to the greater moisture content registered (c.a. about 20% higher) than C-SPC30 films. Despite the higher oxygen permeability of M-SPC30 films compared to SPC films obtained by

pouring method, the OPC of these films were significantly lower than values reported for synthetic polymers. Considering compression molding as a precursor of continuous extrusion process, the results suggest the technical viability of obtaining SPC-based films at large scale by thermo-mechanical methods, with the advantage of using the more economically favorable SPC instead of SPI.

#### Acknowledgment

Authors want to express their gratitude the National Research Council (CONICET, PIP PIP 112-200801-01837) and to ANPCyT (grant number PICT2010-1791) for their financial support.

#### References

- ASTM. (2000). *Standard test methods for water vapor transmission of materials. E96–00*. Philadelphia, PA: American Society for Testing and Materials.
- ASTM. (2002). *Standard test method for oxygen gas transmission rate through plastic film and sheeting using a coulometric sensor. D3985-02*. Philadelphia, PA: American Society for Testing and Materials.
- ASTM. (2002). *Standard test method for tensile properties of plastics by use of microtensile specimens. D1708–02a*. Philadelphia, PA: American Society for Testing and Materials.
- Aydt, T. P., Weller, C., & Testin, R. F. (1991). Mechanical and barrier properties of edible corn and wheat protein films. *Biological Systems Engineering*, 34(1), 207–211.
- Barth, A. (2007). Infrared spectroscopy of proteins. *Biochimica et Biophysica Acta (BBA) – Bioenergetics*, 1767(9), 1073–1101.
- de la Caba, K., Peña, C., Ciannamea, E. M., Stefani, P. M., Mondragon, I., & Ruseckaite, R. A. (2012). Characterization of soybean protein concentrate–stearic acid/palmitic acid blend edible films. *Journal of Applied Polymer Science*, 124(3), 1796–1807.
- Chen, L., & Subirade, M. (2009). Elaboration and characterization of Soy/Zein protein microspheres for controlled nutraceutical delivery. *Biomacromolecules*, 10(12), 3327–3334.
- Chen, P., & Zhang, L. (2005). New evidences of glass transitions and microstructures of soy protein plasticized with glycerol. *Macromolecular Bioscience*, 5(3), 237–245.
- Choi, S. G., Kim, K. M., Hanna, M. A., Weller, C. L., & Kerr, W. L. (2003). Molecular dynamics of soy-protein isolate films plasticized by water and glycerol. *Journal of Food Science*, 68(8), 2516–2522.
- Ciannamea, E. M., Martucci, J. F., Stefani, P. M., & Ruseckaite, R. A. (2012). Bonding quality of chemically-modified soybean protein concentrate-based adhesives in particleboards from Rice Husks. *Journal of the American Oil Chemists' Society*, 89(9), 1733–1741.
- Ciannamea, E. M., Sagüés, F. M., Saumell, C., Stefani, P. M., & Ruseckaite, R. A. (2013). Soybean protein films. Characterization and potential as novel delivery devices of *Duddingtonia flagrans* chlamydozoospores. *Biological Control*, 66(2), 92–101.
- Cunningham, P., Ogale, A. A., Dawson, P. L., & Acton, J. C. (2000). Tensile properties of soy protein isolate films produced by a thermal compaction technique. *Journal of Food Science*, 65(4), 668–671.



- Delassus, P. (1997). Barrier polymers. In A. L. Brody, & K. S. Marsh (Eds.), *The Wiley Encyclopedia of packaging technology* (pp. 71–77). New York: Wiley.
- Denavi, G., Tapia-Blácido, D. R., Añón, M. C., Sobral, P. J. A., Mauri, A. N., & Menegalli, F. C. (2009). Effects of drying conditions on some physical properties of soy protein films. *Journal of Food Engineering*, 90(3), 341–349.
- Gällstedt, M., Mattozzi, A., Johansson, E., & Hedenqvist, M. S. (2004). Transport and tensile properties of compression-molded wheat gluten films. *Biomacromolecules*, 5(5), 2020–2028.
- Garrido, T., Etxabide, A., Peñalba, M., de la Caba, K., & Guerrero, P. (2013). Preparation and characterization of soy protein thin films: processing–properties correlation. *Materials Letters*, 105(0), 110–112.
- Gennadios, A., Brandenburg, A. H., Weller, C. L., & Testin, R. F. (1993). Effect of pH on properties of wheat gluten and soy protein isolate films. *Journal of Agricultural and Food Chemistry*, 41(11), 1835–1839.
- Guckian, S., Dwyer, C., O'Sullivan, M., O'Riordan, E., & Monahan, F. (2006). Properties of and mechanisms of protein interactions in films formed from different proportions of heated and unheated whey protein solutions. *European Food Research and Technology*, 223(1), 91–95.
- Guerrero, P., Retegi, A., Gabilondo, N., & de la Caba, K. (2010). Mechanical and thermal properties of soy protein films processed by casting and compression. *Journal of Food Engineering*, 100(1), 145–151.
- Hager, D. F. (1984). Effects of extrusion upon soy concentrate solubility. *Journal of Agricultural and Food Chemistry*, 32(2), 293–296.
- Hernandez-Izquierdo, V. M., & Krochta, J. M. (2008). Thermoplastic processing of proteins for film formation—a review. *Journal of Food Science*, 73(2), R30–R39.
- Hettiarachchy, N. S., & Eswaranandam, S. (2005). Edible films and coatings from soybean and other protein sources. In *Bailey's industrial oil and fat products*. John Wiley & Sons, Inc.
- Hong, S. I., & Krochta, J. M. (2003). Oxygen barrier properties of whey protein isolate coatings on polypropylene films. *Journal of Food Science*, 68(1), 224–228.
- Janjarasskul, T., & Krochta, J. M. (2010). Edible packaging materials. *Annual Review of Food Science and Technology*, 1(1), 415–448.
- Jiang, J., Xiong, Y. L., Newman, M. C., & Rentfrow, G. K. (2012). Structure-modifying alkaline and acidic pH-shifting processes promote film formation of soy proteins. *Food Chemistry*, 132(4), 1944–1950.
- Kim, K. M., Weller, C. L., Hanna, M. A., & Gennadios, A. (2002). Heat curing of soy protein films at selected temperatures and pressures. *Lebensmittel-Wissenschaft und-Technologie*, 35(2), 140–145.
- Kokoszka, S., Debeaufort, F., Hambleton, A., Lenart, A., & Voilley, A. (2010). Protein and glycerol contents affect physico-chemical properties of soy protein isolate-based edible films. *Innovative Food Science and Emerging Technologies*, 11, 503.
- Krishna, M., Nindo, C. I., & Min, S. C. (2012). Development of fish gelatin edible films using extrusion and compression molding. *Journal of Food Engineering*, 108(2), 337–344.
- Kuktaite, R., Plivelic, T. S. S., Cerenius, Y., Hedenqvist, M. S., Gällstedt, M., Marttila, S., et al. (2011). Structure and morphology of wheat gluten films: from polymeric protein aggregates toward superstructure arrangements. *Biomacromolecules*, 12(5), 1438–1448.
- Kunte, L., Gennadios, A., Cuppett, S., Hanna, M., & Weller, C. (1997). Cast films from soy protein isolates and fractions. *Cereal Chemistry*, 74, 115.
- Lefèvre, T., Subirade, M., & Pézolet, M. (2005). Molecular description of the formation and structure of plasticized globular protein films. *Biomacromolecules*, 6(6), 3209–3219.
- Liu, K., & Hsieh, F.-H. (2008). Protein–Protein interactions during high-moisture extrusion for fibrous meat analogues and comparison of protein solubility methods using different solvent systems. *Journal of Agricultural and Food Chemistry*, 56(8), 2681–2687.
- Lodha, P., & Netravali, A. N. (2005). Thermal and mechanical properties of environment-friendly 'green' plastics from stearic acid modified-soy protein isolate. *Industrial Crops and Products*, 21(1), 49–64.
- Mangavel, C., Rossignol, N., Perronet, A., Barbot, J., Popineau, Y., & Gueguen, J. (2004). Properties and microstructure of thermo-pressed wheat gluten films: a comparison with cast films. *Biomacromolecules*, 5(4), 1596–1601.
- Martucci, J. F., & Ruseckaite, R. A. (2009). Tensile properties, barrier properties, and biodegradation in soil of compression—molded gelatin-dialdehyde starch films. *Journal of Applied Polymer Science*, 112(4), 2166–2178.
- Mauri, A. N., & Añón, M. C. (2006). Effect of solution pH on solubility and some structural properties of soybean protein isolate films. *Journal of the Science of Food and Agriculture*, 86(7), 1064–1072.
- McHugh, T. H., Avena-Bustillos, R., & Krochta, J. M. (1993). Hydrophilic edible films: modified procedure for water vapor permeability and explanation of thickness effects. *Journal of Food Science*, 58(4), 899–903.
- McHugh, T. H., & Krochta, J. M. (1994). Sorbitol- vs glycerol-plasticized whey protein edible films: integrated oxygen permeability and tensile property evaluation. *Journal of Agricultural and Food Chemistry*, 42(4), 841–845.
- Ministry of Agriculture Livestock and Fisheries Argentina. (2013). *Integrated agricultural information*.
- Monahan, F. J., German, J. B., & Kinsella, J. E. (1995). Effect of pH and temperature on protein unfolding and thiol/disulfide interchange reactions during heat-induced gelation of whey proteins. *Journal of Agricultural and Food Chemistry*, 43(1), 46–52.
- Mo, X. Q., & Sun, X. Z. (2002). Plasticization of soy protein polymer by polyol-based plasticizers. *Journal of the American Oil Chemists' Society*, 79(2), 197–202.
- Moore, G. R. P., Martelli, S., Gandolfo, C., Sobral, P. J. A., & Laurindo, J. B. (2006). Influence of the glycerol concentration on some physical properties of feather keratin films. *Food Hydrocolloids*, 20(7), 975–982.
- Ogale, A. A., Cunningham, P., Dawson, P. L., & Acton, J. C. (2000). Viscoelastic, thermal, and microstructural characterization of soy protein isolate films. *Journal of Food Science*, 65(4), 672–679.
- Paetau, I., Chen, C.-Z., & Jane, J.-I. (1994). Biodegradable plastic made from soybean products. 1. Effect of preparation and processing on mechanical properties and water absorption. *Industrial & Engineering Chemistry Research*, 33(7), 1821–1827.
- Park, H. J., & Chinnan, M. S. (1995). Gas and water vapor barrier properties of edible films from protein and cellulosic materials. *Journal of Food Engineering*, 25(4), 497–507.
- Park, J. W., Scott Whiteside, W., & Cho, S. Y. (2008). Mechanical and water vapor barrier properties of extruded and heat-pressed gelatin films. *LWT – Food Science and Technology*, 41(4), 692–700.
- Reddy, N., & Yang, Y. (2013). Thermoplastic films from plant proteins. *Journal of Applied Polymer Science*, 130(2), 729–738.
- Rhim, J. W., Gennadios, A., Handa, A., Weller, C. L., & Hanna, M. A. (2000). Solubility, tensile, and color properties of modified soy protein isolate films. *Journal of Agricultural and Food Chemistry*, 48(10), 4937–4941.
- Rhim, J. W., Gennadios, A., Weller, C. L., Carole, C., & Hanna, M. A. (1998). Soy protein isolate-dialdehyde starch films. *Industrial Crops and Products*, 8(3), 195–203.
- Singh, P., Kumar, R., Sabapathy, S. N., & Bawa, A. S. (2008). Functional and edible uses of soy protein products. *Comprehensive Reviews in Food Science and Food Safety*, 7(1), 14–28.
- Song, F., Tang, D.-L., Wang, X.-L., & Wang, Y.-Z. (2011). Biodegradable soy protein isolate-based materials: a review. *Biomacromolecules*, 12(10), 3369–3380.
- Sothornvit, R., & Krochta, J. M. (2001). Plasticizer effect on mechanical properties of [beta]-lactoglobulin films. *Journal of Food Engineering*, 50(3), 149–155.
- Sothornvit, R., Olsen, C. W., McHugh, T. H., & Krochta, J. M. (2003). Formation conditions, water-vapor permeability, and solubility of compression-molded whey protein films. *Journal of Food Science*, 68(6), 1985–1999.
- Sothornvit, R., Olsen, C. W., McHugh, T. H., & Krochta, J. M. (2007). Tensile properties of compression-molded whey protein sheets: determination of molding condition and glycerol-content effects and comparison with solution-cast films. *Journal of Food Engineering*, 78(3), 855–860.
- Stuchell, Y. M., & Krochta, J. M. (1995). Edible Coatings on frozen king Salmon: effect of whey protein isolate and acetylated monoglycerides on moisture loss and lipid oxidation. *Journal of Food Science*, 60(1), 28–31.
- Sun, S., Song, Y., & Zheng, Q. (2008). Thermo-molded wheat gluten plastics plasticized with glycerol: effect of molding temperature. *Food Hydrocolloids*, 22(6), 1006–1013.
- Sun, Q., Wang, P., Lei, H., Han, D., Feng, P., Wu, H., et al. (2009). Characteristics of soy protein isolate films modified by glycerol and oleic acid. *Food Science*, 30(15), 52–58.
- Ullsten, N. H., Cho, S.-W., Spencer, G., Gällstedt, M., Johansson, E., & Hedenqvist, M. S. (2009). Properties of extruded vital wheat gluten sheets with sodium hydroxide and salicylic acid. *Biomacromolecules*, 10(3), 479–488.
- Ustunol, Z., & Mert, B. (2004). Water solubility, mechanical, barrier, and thermal properties of cross-linked whey protein isolate-based films. *Journal of Food Science*, 69(3), FEP129–FEP133.